Published in final edited form as:
Nature. 2010 October 21; 467(7318): 986–990. doi:10.1038/nature09459.

TAp63 suppresses metastasis through coordinate regulation of *Dicer* and miRNAs

Xiaohua Su[1,*], **Deepavali Chakravarti**[1,2,*], **Min Soon Cho**[1,2], **Lingzhi Liu**[1], **Young Jin Gi**[1], **Yu-Li Lin**[1], **Marco L. Leung**[1], **Adel El-Naggar**[3], **Chad J. Creighton**[4], **Milind B. Suraokar**[3], **Ignacio Wistuba**[3], and **Elsa R. Flores**[1,2]

[1]Department of Molecular and Cellular Oncology, The University of Texas M. D. Anderson Cancer Center, 1515 Holcombe Boulevard, Houston, Texas 77030, USA

[2]Graduate School of Biomedical Sciences, The University of Texas M. D. Anderson Cancer Center, 1515 Holcombe Boulevard, Houston, Texas 77030, USA

[3]Department of Pathology, The University of Texas M. D. Anderson Cancer Center, 1515 Holcombe Boulevard, Houston, Texas 77030, USA

[4]Dan L. Duncan Cancer Center, Baylor College of Medicine, Houston, Texas 77030, USA

Abstract

Aberrant expression of microRNAs (miRNAs) and the enzymes that control their processing have been reported in multiple biological processes including primary and metastatic tumours[1–6], but the mechanisms governing this are not clearly understood. Here we show that TAp63, a p53 family member, suppresses tumorigenesis and metastasis, and coordinately regulates *Dicer* and *miR-130b* to suppress metastasis. Metastatic mouse and human tumours deficient in TAp63 express Dicer at very low levels, and we found that modulation of expression of *Dicer* and *miR-130b* markedly affected the metastatic potential of cells lacking *TAp63*. TAp63 binds to and transactivates the *Dicer* promoter, demonstrating direct transcriptional regulation of *Dicer* by TAp63. These data provide a novel understanding of the roles of TAp63 in tumour and metastasis suppression through the coordinate transcriptional regulation of *Dicer* and *miR-130b* and may have implications for the many processes regulated by miRNAs.

The precise roles of *p63* in tumour suppression have been hotly debated[7–10]. Although some studies show p63 overexpression in human cancer[7,8,11], some demonstrate a loss of p63 associated with tumour progression and metastasis8,12–14. Much of this controversy is due to the existence of multiple isoforms15. The full-length TA isoform of p63 bears structural and functional similarity to p53, whereas the ΔN isoforms of p63, which lack the transactivation (TA) domain, act primarily in dominant-negative fashion against p53, TAp63

Correspondence and requests for materials should be addressed to E.R.F. (elsaflores@mdanderson.org).
*These authors contributed equally to this work.

Supplementary Information is linked to the online version of the paper at www.nature.com/nature.

Author Contributions X.S., D.C. and E.R.F. designed the experiments and analysed the data. X.S., D.C., M.S.C., L.L., Y.J.G., Y.-L.L. and M.L.L. performed the experiments. A.E.-N. performed pathology analysis and provided human HNSCC samples. M.B.S. and I.W. provided human lung adenocarcinoma pathology information and RNA samples. C.J.C. performed statistical analysis on miRNA data. X.S., D.C. and E.R.F. wrote the manuscript. All authors discussed the results and commented on the manuscript.

The authors declare no competing financial interests.

Readers are welcome to comment on the online version of this article at www.nature.com/nature.

and TAp73 (ref. 15). These activities suggest that *TAp63* is a tumour suppressor gene and Δ*Np63* is an oncogene; however, this has not been directly tested *in vivo*. To examine whether *TAp63* is a tumour suppressor gene, we generated a cohort of 30 mice of each of the following genotypes: $TAp63^{-/-}$, $TAp63^{+/-}$ and wild-type, and aged them for 2.5 years (Fig. 1 and Supplementary Fig. 1a, b). We found that both $TAp63^{+/-}$ mice and $TAp63^{-/-}$ mice developed spontaneous carcinomas and sarcomas (Fig. 1a–d, Supplementary Fig. 1a, b, and Supplementary Table 1) and had a significantly shorter lifespan than the wild-type cohort (Fig. 1c). Paradoxically, we noted that a larger proportion of the $TAp63^{-/-}$ mice (24%) were tumour free compared with $TAp63^{+/-}$ mice (15%) (Fig. 1c, d). These data suggest that *TAp63* is a haploinsufficient tumour suppressor gene. Consistent with this finding, sarcomas ($n = 10$) and carcinomas ($n = 10$) from $TAp63^{+/-}$ mice retained the wild-type allele of *TAp63* (Fig. 1e). $TAp63^{+/-}$ and $TAp63^{-/-}$ mice developed highly metastatic tumours (Fig. 1a, b, f, and Supplementary Fig. 1a, b), and 10% of these metastases were found in the brain (Fig. 1b), a rare finding in spontaneous mouse tumour models. Although equivalent numbers of carcinomas metastasized in the $TAp63^{-/-}$ and $TAp63^{+/-}$ mice, a greater number of sarcomas metastasized in $TAp63^{+/-}$ mice than in $TAp63^{-/-}$ mice (Fig. 1f, g). These data again indicate that heterozygosity for *TAp63* results in a more severe phenotype in specific tissues.

To further understand the mechanisms employed by *TAp63* as a tumour suppressor gene, we studied the effects of *TAp63* on a $p53^{+/-}$ or $p53^{-/-}$ background[8,16–18]. Some human tumours show alterations in both *p53* and *p63* (refs 12, 13), and point mutant p53 binds and functionally inactivates p63 (refs 17, 18). To study these interactions, we generated six cohorts of 30 mice each: $TAp63^{-/-}$;$p53^{+/-}$ and $TAp63^{+/-}$;$p53^{+/-}$ for comparison with $p53^{+/-}$ mice, and $TAp63^{-/-}$;$p53^{-/-}$ and $TAp63^{+/-}$;$p53^{-/-}$ for comparison with $p53^{-/-}$ mice. Unlike $p53^{+/-}$ and $p53^{-/-}$ mice, *TAp63/p53* compound mutant mice developed a remarkable number of metastatic tumours (Fig. 1h–k, Supplementary Fig. 1c–f and Supplementary Table 1)[8,16]. Whereas the $TAp63^{+/-}$;$p53^{+/-}$ mice had a similar tumour spectrum to that of $TAp63^{-/-}$;$p53^{+/-}$ mice (Supplementary Table 1), the sarcomas of the $TAp63^{+/-}$;$p53^{+/-}$ mice were significantly more invasive and metastatic (88%) than those in the $TAp63^{-/-}$;$p53^{+/-}$ cohort (14%) (Fig. 1k). In contrast, the carcinomas in the $TAp63^{-/-}$;$p53^{+/-}$ cohort were more metastatic (44%) than those in the $TAp63^{+/-}$;$p53^{+/-}$ group (29%) (Fig. 1k). We next examined sarcomas ($n = 10$) and carcinomas ($n = 10$) from $TAp63^{+/-}$;$p53^{+/-}$ mice and found that the wild-type allele of *TAp63* was retained (Fig. 1l). We also examined $TAp63^{+/-}$;$p53^{+/-}$ tumours and $TAp63^{-/-}$;$p53^{+/-}$ tumours for p53 loss of heterozygosity (LOH) and found that one out of ten sarcomas showed LOH of *p53* in $TAp63^{+/-}$;$p53^{+/-}$ tumours (Fig. 1m). A slightly higher frequency was noted in tumours from $TAp63^{-/-}$;$p53^{+/-}$ sarcomas (one out of eight) and carcinomas (two out of eight), indicating that there is increased selective pressure to lose the wild-type *p53* allele in the complete absence of *TAp63* (Fig. 1m). However, the frequency of *p53* LOH was lower than the previously reported frequency (ranging from 75–90%) of sarcomas from $p53^{+/-}$ mice[8,16] and was more reminiscent of the frequency of *p53* LOH in mouse models of Li–Fraumeni syndrome[17], further supporting the concept that p53 and p63 interact in tumour suppression. We also analysed $TAp63^{-/-}$;$p53^{-/-}$ and $TAp63^{+/-}$;$p53^{-/-}$ mice and found that highly metastatic carcinomas and sarcomas developed in addition to the thymic lymphomas found in the $p53^{-/-}$ mice (Fig. 1j and Supplementary Table 1). Sarcomas ($n = 5$) and carcinomas ($n = 5$) from these mice retained the wild-type allele of *TAp63* (Fig. 1l), providing further evidence that *TAp63* is a haploinsufficient tumour suppressor gene.

To understand how heterozygosity of *TAp63* led to a more severe tumour phenotype than a complete loss of *TAp63*, we examined whether senescence in the $TAp63^{-/-}$ mice, which age prematurely[19], inhibited tumorigenesis or metastasis. We found several examples of $TAp63^{-/-}$;$p53^{+/-}$ mice that developed non-metastatic osteosarcomas together with metastatic carcinomas (Fig. 2a, b and Supplementary Fig. 1e, f). Tumours from these mice,

along with sarcomas and carcinomas from *TAp63*$^{+/-}$;*p53*$^{+/-}$ mice, were assayed for senescence-associated markers, namely SA-β-gal (Fig. 2c and Supplementary Fig. 2a, b) or *PML* (encoding promyelocytic leukemia protein), *p16*^{Ink4a} and *p19*^{Arf} (Fig. 2d). We found that osteosarcomas and rhabdomyosarcomas in the *TAp63*$^{-/-}$;*p53*$^{+/-}$ mice expressed high levels of senescence markers, whereas the same tumour types in the *TAp63*$^{+/-}$;*p53*$^{+/-}$ mice did not (Fig. 2c, d). None of the carcinomas from *TAp63*$^{-/-}$;*p53*$^{+/-}$ or *TAp63*$^{+/-}$;*p53*$^{+/-}$ mice was positive for these markers, indicating that *TAp63* deficiency has a tissue-specific function in the induction of senescence. These results correlated with the level of aggressiveness and metastatic potential of these tumours.

Genomic instability in tissues of *TAp63*$^{-/-}$ mice has been shown to be high[19]. To examine whether there is a similarly high level of genomic instability in tumours from *TAp63*$^{-/-}$;*p53*$^{+/-}$ mice and whether this is correlated with tumour aggressiveness and metastasis, we performed γ-H2AX immunostaining and metaphase spreads on tumours from *TAp63* mutant mice (Fig. 2e, f and Supplementary Fig. 2c–g). We did indeed find that *TAp63*$^{-/-}$ carcinomas showed high levels of γ-H2AX, polyploid cells and chromosomal aberrations, suggesting that carcinomas lacking *TAp63* overcome senescence in epithelial tissues as a result of the acquisition of further genetic alterations. Although a decrease in *TAp63* expression promotes metastasis in both tumour types, senescence is triggered in sarcomas, thus inhibiting progression, whereas in carcinomas, genomic instability ensues, permitting further genetic events favouring tumour progression.

Given the high level of metastasis in *TAp63*$^{-/-}$ mice, we examined whether *TAp63*$^{-/-}$ mouse embryonic fibroblasts (MEFs) had an enhanced invasive ability. *TAp63*$^{-/-}$ MEFs showed a 1.8-fold increase in invasion (Fig. 2g). To assess whether this finding could be generalized to human tumours, we examined primary human head and neck squamous-cell carcinomas (HNSCCs) (cell lines 10A, 17A and 22A) and matched metastatic lesions with markedly low levels of *TAp63* (Fig. 2h) (cell lines 10B, 17B and 22B)[20]. Tumours with low levels of *TAp63* showed an increased invasive ability (Fig. 2i), indicating that *TAp63* is a critical regulator of cancer metastasis.

Our findings that *TAp63*$^{+/-}$ tumours are more aggressive than those from *TAp63*$^{-/-}$ mice are reminiscent of the phenotype of *Dicer* conditional knock out (*Dicer1*$^{fl/+}$) mice intercrossed to the *Kras*$^{LSL\text{-}G12D}$ lung cancer model[21], which indicate that *Dicer* is haploinsufficient for tumour suppression[4], in a similar manner to our previous observations for *TAp63*. Additionally, *Dicer1*$^{-/-}$ mice show embryonic lethality (before embryonic day E8.5) similar to that in *TAp63*$^{-/-}$ mice on an enriched C57BL/6 background[19]; 35% of *TAp63*$^{-/-}$ embryos die between E6.5 and E8.5. Given these similarities, we examined whether messenger RNA levels of *Dicer* are dysregulated in tumours and cells lacking *TAp63*. *TAp63*$^{-/-}$ osteosarcomas, lung adenocarcinomas and mammary adenocarcinomas (n = 6) and MEFs expressed significantly lower levels of *Dicer* than *p53*$^{-/-}$ tumours and MEFs (Fig. 3a, b and Supplementary Fig. 3), suggesting that *TAp63* is required for the transcription of *Dicer*. Similarly, we found that metastatic human HNSCCs (n = 46), lung adenocarcinomas and squamous cell carcinomas (n = 92) and mammary adenocarcinomas (n = 43) with low levels of TAp63 had low Dicer expression (Fig. 3c, Supplementary Fig. 4 and Supplementary Tables 2 and 3). These data indicate a critical role for TAp63 in the regulation of *Dicer* in metastasis in human cancer. Consistent with this is the observation that Dicer and Drosha levels have been shown to be low in human cancer[20].

To determine whether *Dicer* is a transcriptional target of TAp63, we performed chromatin immunoprecipitation (ChIP) analysis for a site matching the p63 consensus binding site (Supplementary Table 4). We found that p63, and not p53, bound to the *Dicer* promoter (Fig. 3d and Supplementary Fig. 5a), suggesting that *Dicer* is a direct transcriptional target

of p63. In addition, all isoforms of *TAp63* (α, β and γ) were able to transactivate a *Dicer–luciferase* reporter gene with the p63-binding site (Fig. 3e), further indicating that TAp63 regulates *Dicer* transcriptionally.

To understand whether TAp63 controls metastasis through transcriptional regulation of *Dicer*, we re-expressed *Dicer* in *TAp63*$^{-/-}$ MEFs (Fig. 3f). These cells lost their ability to invade (Fig. 3g). Conversely, wild-type MEFs expressing a *Dicer* short hairpin RNA (shRNA)[22] (Fig. 3f) showed increased invasiveness (Fig. 3h). These data indicate that low levels of *Dicer* lead to increased cell invasion, similar to that observed in *TAp63*-deficient cells.

To further explore the connection between TAp63 and Dicer in metastasis, we modulated levels of *TAp63* in MEFs by expressing *TAp63*γ in *TAp63*$^{-/-}$ MEFs and human HNSCCs (Supplementary Figs 5b and 6a) and measured *Dicer* expression and invasion potential. Levels of *Dicer* increased to wild-type levels in *TAp63*$^{-/-}$ cells expressing *TAp63*γ (Fig. 3i and Supplementary Fig. 6b), which resulted in decreased invasion potential (Fig. 3j and Supplementary Fig. 6c). We also acutely deleted *TAp63* after the introduction of adenovirus-Cre in *TAp63*$^{fl/fl}$ MEFs (Supplementary Fig. 5c). These *TAp63*$^{\Delta/\Delta}$ MEFs showed concomitant downregulation of *Dicer* (Fig. 3k) and a twofold increase in cellular invasion (Fig. 3l), indicating that regulation of *Dicer* by *TAp63* is critical in the suppression of invasion.

Because Dicer expression is low in the absence of TAp63, we assessed the processing of miRNAs that have a recognized role in lung and mammary adenocarcinoma metastasis[1–3,23], namely miR-10b, miR-200b, miR200c, miR34a and miR-130b, in *TAp63*$^{-/-}$ MEFs and found that their processing is defective (Fig. 3m). To examine whether modulating levels of TAp63 in cells would affect miRNA processing, we scored for processing of miR-10b in *TAp63*$^{-/-}$ MEFs reconstituted with *TAp63*γ and in *TAp63*-ablated (*TAp63*$^{\Delta/\Delta}$) MEFs. When TAp63 was re-expressed, we observed a rescue of miRNA processing, and when *TAp63* was acutely deleted, we observed a diminution of miRNA processing (Fig. 3n). The precursor of miR-130b (pre-miR-130b) was present at low levels in *TAp63*$^{-/-}$ MEFs (Fig. 3o), indicating that the primary transcript of *miR-130b* may be expressed at low levels in the absence of TAp63.

We found that levels of *miR-130b* were downregulated in *TAp63*$^{-/-}$ MEFs, suggesting a role for TAp63 in its regulation (Fig. 4a). We reasoned that other miRNAs, such as *miR-34a*, which have been shown to be a transcriptional target of p53 (ref. 23), may also be a target of TAp63. Indeed, *miR-130b* and *miR-34a* were downregulated in the absence of TAp63 (Fig. 4a–c and Supplementary Fig. 7a). *miR130b* was also low in high-grade lung adenocarcinomas and HNSCCs with low levels of *TAp63* and *Dicer* (Supplementary Table 3). To assess whether p63 binds to the promoters of these miRNAs, we performed a ChIP analysis with identified putative p63-binding sites (Supplementary Table 4). We found a significant level of p63 binding at both the *miR-130b* and *miR-34a* promoters (Fig. 4d and Supplementary Fig. 7b–d). To determine whether p63 can directly transactivate *miR-130b* and *miR-34a*, we performed luciferase assays (Fig. 4e and Supplementary Fig. 7e) and found that TAp63 transactivated the *miR130b* reporter. We modulated the levels of TAp63 by overexpression or acute deletion in MEFs and found that levels of *miR-130b* correlated with levels of *TAp63* (Fig. 4f, g). Taken together, these data indicate that *miR-130b* is a direct target of TAp63.

To understand whether regulation of *miR-130b* by TAp63 has a function in the metastatic phenotype, we modulated levels of *miR-130b* in MEFs (Supplementary Fig. 7f–h) and assessed invasion (Fig. 4h, i). Wild-type MEFs with low levels of *miR-130b* showed

increased invasion (Fig. 4h), and *TAp63*$^{-/-}$ MEFs expressing both *miR-130b* and *Dicer* showed decreased invasion (Fig. 4i) comparable to that of wild-type MEFs. This suggests that coordinate regulation of both *Dicer* and *miR-130b* by TAp63 is critical in suppressing metastasis.

We have shown that TAp63 is a suppressor of tumorigenesis and metastasis and that its complete inactivation results in tissue-specific antagonistic pleiotropy with respect to tumour progression including genomic instability and activation of senescence. Both the spectrum and the highly metastatic nature of tumours in *TAp63*-deficient mice are consistent with a role for TAp63 as a master regulator of metastasis. Furthermore, we have shown a role for transcriptional regulation by TAp63 of *Dicer* and *miR-130b* in metastasis. Given the diverse biological roles of both Dicer and TAp63, a complete understanding of the regulation of *Dicer* by TAp63 in other processes is a key question for the future.

METHODS SUMMARY

Generation of mice and tumour analysis

TAp63$^{-/-}$ mice[19] were intercrossed with *p53*$^{-/-}$ mice[16] to generate compound mutant *TAp63/p53* mice on an enriched C57BL/6 background ((C57BL/6 = 95%) and (129/SvJae = 5%)). For analysis of tumour formation and metastatic disease, 30 mice of each genotype were aged for 2.5 years. Moribund mice were killed, following the approved guidelines of the IACUC at the University of Texas M. D. Anderson Cancer Center and analysed histologically by haematoxylin/eosin (H&E) staining as described previously[8]. Tumour-free survival of mice was plotted with PRISM5 software (GraphPad).

Migration and invasion assay

MEFs or mouse and human tumour cell lines were resuspended in 500 μl of DMEM with 10% FBS and 1 × penicillin/streptomycin (5×10^4 cells) and added to the top of each chamber containing BD BioCoat cell culture inserts (354578; BD Biosciences) or Matrigel Invasion Chamber (354480; BD Biosciences)[19,24]. Non-invasive cells were removed from the upper chamber. Cells remaining on the membrane were fixed, stained with Diff-Quik (Dade Behring, Inc.), and counted with a Zeiss AxioObserver A1 inverted microscope.

Full Methods and any associated references are available in the online version of the paper at www.nature.com/nature.

Supplementary Material

Refer to Web version on PubMed Central for supplementary material.

Acknowledgments

We thank C.-g. Liu for technical assistance with miRNA analyses and A. Multani for metaphase analyses (funded by NCI CA16672); K. Y. Tsai for scientific discussions and comments on the manuscript; and D. Yu, J. Jackson and S. Rehman for reagents and advice. This work was supported by grants to E.R.F. from the American Cancer Society (RSG-07-082-01-MGO), the Susan G. Komen Foundation (BCTR600208) and the Hildegardo E. and Olga M. Flores Foundation. This work was supported in part by an NCI-Cancer Center Core Grant (CA-16672) (University of Texas M. D. Anderson Cancer Center), a Career Development Award from the Genitourinary Cancer SPORE (P50CA091846) to E.R.F., Lung Cancer SPORE (P50CA070907) to I.W. and U01DE019765 to A.E.-N. E.R.F. is a scholar of the Rita Allen Foundation and the V Foundation for Cancer Research.

References

1. Baffa R, et al. MicroRNA expression profiling of human metastatic cancers identifies cancer gene targets. J. Pathol 2009;219:214–221. [PubMed: 19593777]

2. Gibbons DL, et al. Contextual extracellular cues promote tumor cell EMT and metastasis by regulating miR-200 family expression. Genes Dev 2009;23:2140–2151. [PubMed: 19759262]
3. Ma L, Teruya-Feldstein J, Weinberg RA. Tumour invasion and metastasis initiated by microRNA-10b in breast cancer. Nature 2007;449 682-628.
4. Kumar MS, et al. *Dicer1* functions as a haploinsufficient tumor suppressor. Genes Dev 2009;23:2700–2704. [PubMed: 19903759]
5. Lu J, et al. MicroRNA expression profiles classify human cancers. Nature 2005;435:834–838. [PubMed: 15944708]
6. Merritt WM, et al. Dicer, Drosha, and outcomes in patients with ovarian cancer. N. Engl. J. Med 2008;359:2641–2650. [PubMed: 19092150]
7. Flores ER. The roles of *p63* in cancer. Cell Cycle 2007;6:300–304. [PubMed: 17264676]
8. Flores ER, et al. Tumor predisposition in mice mutant for *p63* and *p73*: evidence for broader tumor suppressor functions for the *p53* family. Cancer Cell 2005;7:363–373. [PubMed: 15837625]
9. Keyes WM, et al. *p63* heterozygous mutant mice are not prone to spontaneous or chemically induced tumors. Proc. Natl Acad. Sci. USA 2006;103:8435–8440. [PubMed: 16714381]
10. Yang A, Kaghad M, Caput D, McKeon F. On the shoulders of giants: p63, p73 and the rise of p53. Trends Genet 2002;18:90–95. [PubMed: 11818141]
11. Hibi K, et al. *AIS* is an oncogene amplified in squamous cell carcinoma. Proc. Natl Acad. Sci. USA 2000;97:5462–5467. [PubMed: 10805802]
12. Park BJ, et al. Frequent alteration of *p63* expression in human primary bladder carcinomas. Cancer Res 2000;60:3370–3374. [PubMed: 10910040]
13. Urist MJ, et al. Loss of *p63* expression is associated with tumor progression in bladder cancer. Am. J. Pathol 2002;161:1199–1206. [PubMed: 12368193]
14. Park HR, et al. Low expression of *p63* and *p73* in osteosarcoma. Tumori 2004;90:239–243. [PubMed: 15237589]
15. Yang A, et al. *p63*, a *p53* homolog at 3q27-29, encodes multiple products with transactivating, death-inducing, and dominant-negative activities. Mol. Cell 1998;2:305–316. [PubMed: 9774969]
16. Jacks T, et al. Tumor spectrum analysis in *p53*-mutant mice. Curr. Biol 1994;4:1–7. [PubMed: 7922305]
17. Lang GA, et al. Gain of function of a p53 hot spot mutation in a mouse model of Li-Fraumeni syndrome. Cell 2004;119:861–872. [PubMed: 15607981]
18. Olive KP, et al. Mutant *p53* gain of function in two mouse models of Li-Fraumeni syndrome. Cell 2004;119:847–860. [PubMed: 15607980]
19. Su X, et al. *TAp63* prevents premature aging by promoting adult stem cell maintenance. Cell Stem Cell 2009;5:64–75. [PubMed: 19570515]
20. Maruya S, et al. Differential methylation status of tumor-associated genes in head and neck squamous carcinoma: incidence and potential implications. Clin. Cancer Res 2004;10:3825–3830. [PubMed: 15173091]
21. Jackson EL, et al. Analysis of lung tumor initiation and progression using conditional expression of oncogenic K-ras. Genes Dev 2001;15:3243–3248. [PubMed: 11751630]
22. Kumar MS, et al. Impaired microRNA processing enhances cellular transformation and tumorigenesis. Nature Genet 2007;39:673–677. [PubMed: 17401365]
23. He L, et al. A microRNA component of the p53 tumour suppressor network. Nature 2007;447:1130–1134. [PubMed: 17554337]
24. Flores ER, et al. p63 and p73 are required for p53-dependent apoptosis in response to DNA damage. Nature 2002;416:560–564. [PubMed: 11932750]

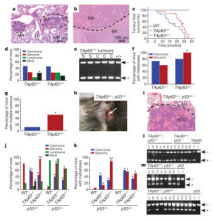

Figure 1. *TAp63*$^{-/-}$ mice develop metastatic tumours

a, b, Metastatic mammary adenocarcinoma in lung (LU; **a**) and brain (BR; **b**). **c**, Tumour-free survival curves; $n = 30$ and $P \leq 0.05$. WT, wild type. **d**, Tumour spectra of the indicated mice genotypes; $n = 30$. **e**, LOH analysis of *TAp63* in sarcomas (S) and carcinomas (C) from the indicated genotypes. **f, g**, Percentage of metastatic sarcomas and carcinomas (**f**) and multiple malignancies (**g**); $n = 30$. **h, i**, Metastatic squamous cell carcinoma (SCC) on skin (**h**) and in lung (LU; **i**). **j, k**, Tumour spectrum (**j**) and metastases (**k**) of the indicated mice genotypes; $n = 30$. Asterisk, statistical difference between *TAp63/p53* mutant and *p53*$^{+/-}$ or *p53*$^{-/-}$ mice; two asterisks, statistical difference between two double-mutant genotypes; $P \leq 0.05$. **l, m**, PCR analysis for LOH of *TAp63* (**l**) or p53 (**m**) in carcinomas (C) and sarcomas (S) of the indicated genotypes.

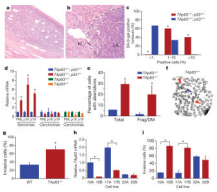

Figure 2. *TAp63*-deficient tumours show high levels of senescence and genomic instability

a, b, Non-metastatic osteosarcoma (**a**) and metastatic lung adenocarcinoma (LA) in kidney (KI) (**b**) from $TAp63^{-/-};p53^{+/-}$ mouse. **c**, Percentage of SA-β-gal-positive sarcomas; $n = 6$ of each genotype. **d**, Quantitative real-time polymerase chain reaction (qRT-PCR) for markers of senescence (*PML*, $p16^{Ink4a}$ and $p19^{Arf}$) in the indicated tumours; $n = 6$ of each genotype. **e**, Percentage of $TAp63^{-/-}$ and $TAp63^{+/-}$ tumours with chromosomal aberrations determined by metaphase spreads; $n = 6$ of each genotype. Frag/DM, fragmented, double-minute chromosome. **f**, Representative metaphase spread from a $TAp63^{-/-}$ tumour. Coloured arrows indicate aberrations: rings (red arrows) and double minutes (blue arrow). **g**, Invasion assays in wild-type MEFs ($n = 3$) and $TAp63^{-/-}$ MEFs ($n = 3$). **h**, qRT-PCR for *TAp63* in the indicated human squamous cell carcinoma (HNSCC) cell lines; $n = 5$. **i**, Invasion assays in HNSCC cell lines; $n = 5$. Error bars indicate s.e.m. Asterisk, $P \leq 0.05$.

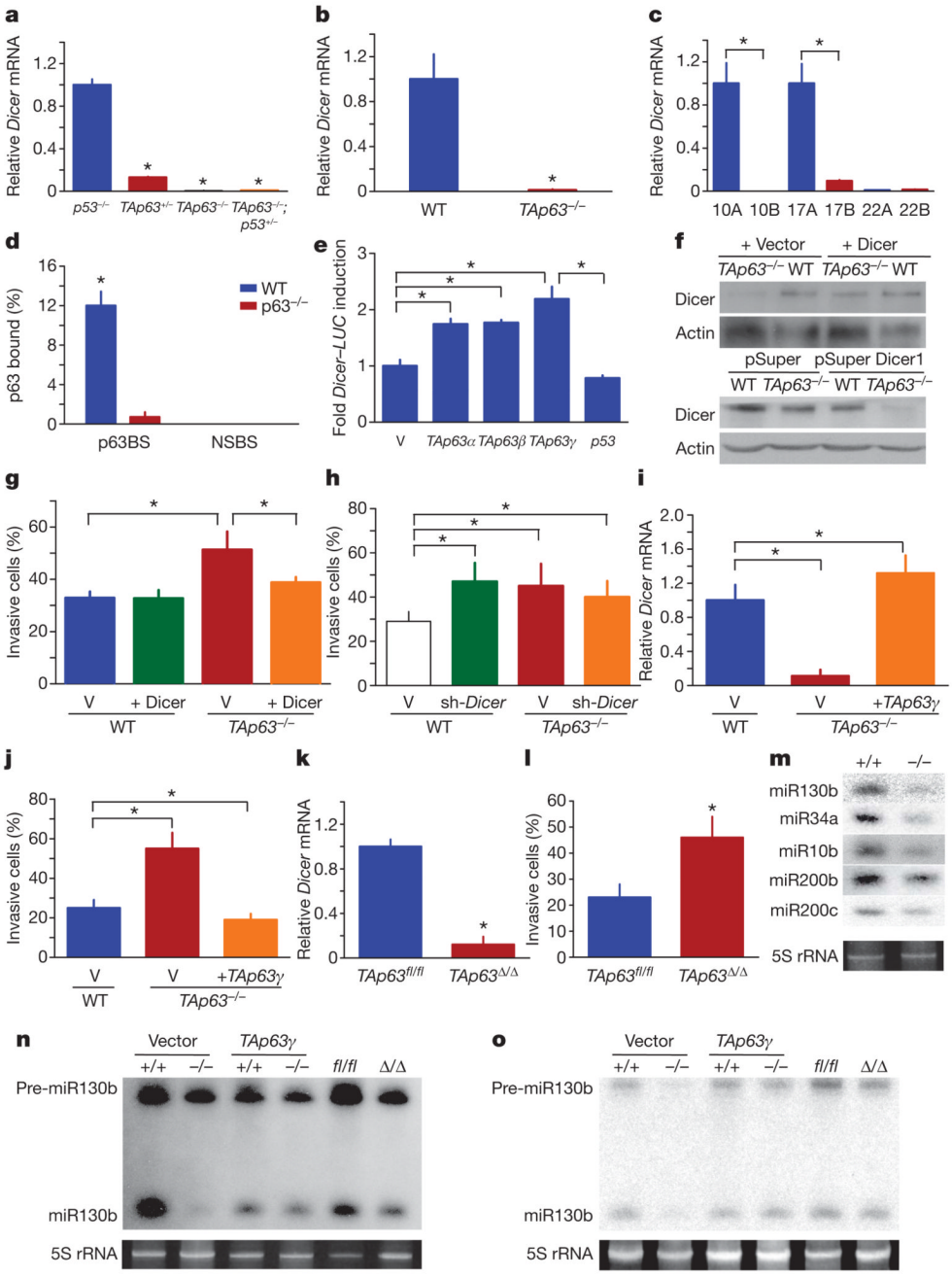

Figure 3. TAp63 regulates metastasis by transcriptional activation of *Dicer*

a–c, qRT-PCR of *Dicer* mRNA in murine tumours (**a**), MEFs (**b**) and HNSCC cell lines (**c**); *n* = 5. **d**, qRT-PCR of ChIP assay using keratinocytes and indicating p63-binding site (p63BS) and nonspecific binding site (NSBS) on *Dicer* promoter; *n* = 3. **e**, Luciferase assay for *Dicer*; *n* = 5. V, pcDNA3 vector. **f**, Western blot analysis for Dicer expression in MEFs infected with the indicated vectors. **g, h**, Invasion assays of MEFs expressing *Dicer* (**g**) and MEFs expressing shRNA-*Dicer* (**h**); *n* = 3. **i**, qRT-PCR for *Dicer* in MEFs expressing *TAp63*γ; *n* = 3. **j**, Invasion assays of MEFs expressing *TAp63*γ; *n* = 3. **k**, qRTPCR for *Dicer* in wild-type (*TAp63*$^{fl/fl}$) and *TAp63*-ablated (*TAp63*$^{\Delta/\Delta}$) MEFs; *n* = 3. **l**, Invasion assays of *TAp63*$^{\Delta/\Delta}$ MEFs; *n* = 3. **m**, Northern blot analysis for the indicated mature miRNAs in wild-

type and *TAp63*$^{-/-}$ MEFs. **n, o**, Northern blot analysis for miR-10b (**n**) or miR-130b (**o**) using MEFs of the indicated genotypes expressing vector (V) or *TAp63*γ. Error bars indicate s.e.m. Asterisk, $P \leq 0.05$.

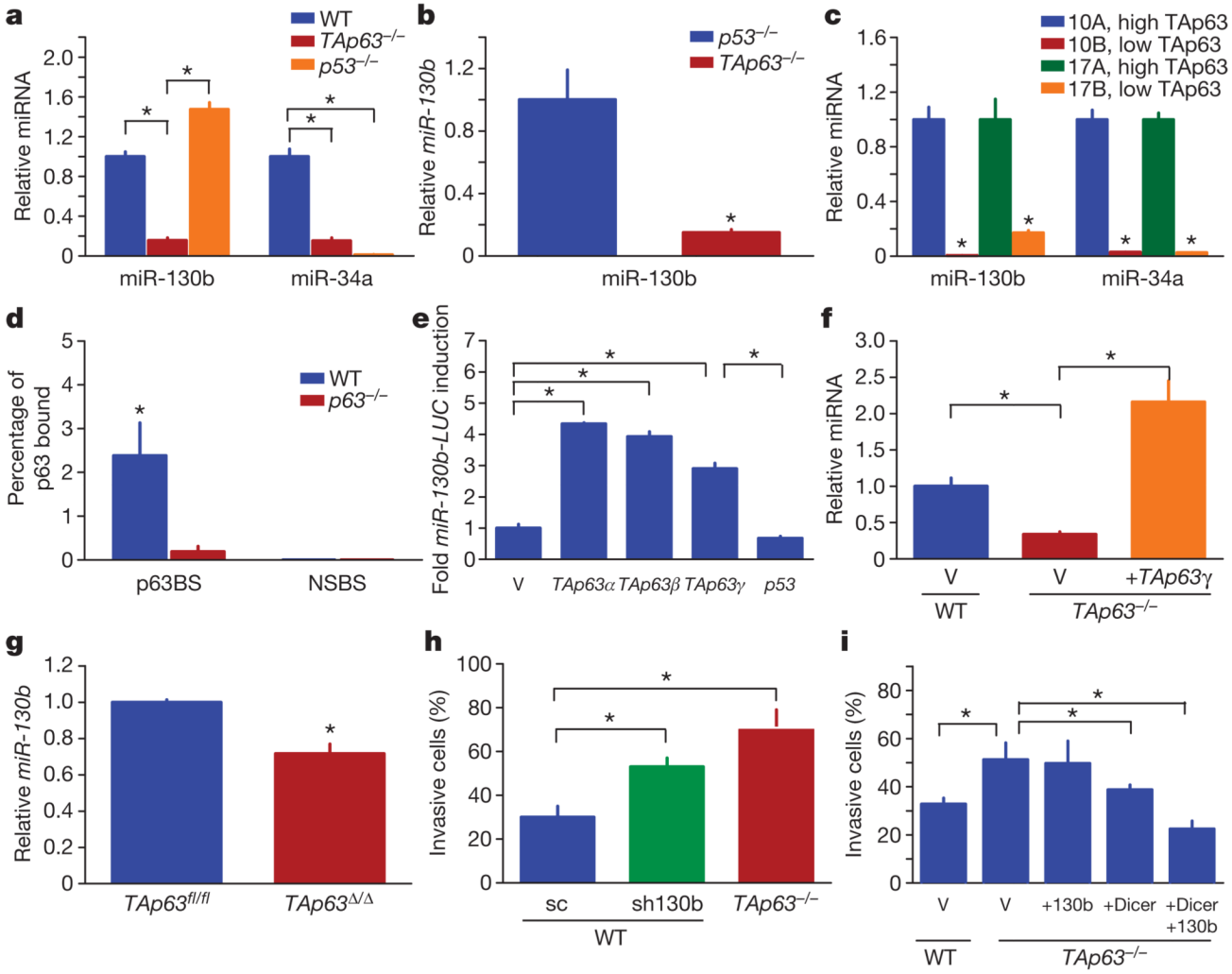

Figure 4. *TAp63* regulates *miR-130b* in metastasis

a–c, TaqMan reverse-transcriptase-mediated PCR (RT–PCR) for *miR-130b* and *miR-34a* in MEFs (**a**), murine tumours (**b**) and HNSCCs (**c**); $n = 5$. **d**, qRT-PCR of ChIP assay for *miR-130b* indicating p63-binding site (p63BS) and non-specific binding site (NSBS); $n = 3$. **e**, Luciferase assay for *miR-130b*; $n = 3$. **f, g**, TaqMan RT–PCR for *miR-130b* in wild-type and $TAp63^{-/-}$ MEFs expressing the indicated vectors (**f**) and wild-type ($TAp63^{fl/fl}$) and *TAp63*-ablated ($TAp63^{\Delta/\Delta}$) MEFs (**g**); $n = 3$. **h, i**, Invasion assays of MEFs infected with shRNA-miR-130b (sh-130b) (**h**) and wild-type and $TAp63^{-/-}$ MEFs expressing the indicated vectors (**i**); $n = 3$. Scrambled sequence (sc) shRNA was used as a negative control. Error bars indicate s.e.m. Asterisk, $P \leq 0.05$.